NbN HOT-ELECTRON MIXER AT RADIATION FREQUENCIES BETWEEN 0.9 THz AND 1.2 THz

Yu.P. Gousev* and H.K. Olsson
Royal Institute of Technology, S-164 40 Kista-Stockholm, Sweden

G.N. Gol'tsman, B.M. Voronov, and E.M. Gershenzon,
Moscow State Pedagogical University, 117 439 Moscow, Russia

We report on noise temperature measurements for a NbN phonon-cooled hot-electron mixer at radiation frequencies between 0.9 THz and 1.2 THz. Radiation was coupled to the mixer, placed in a vacuum chamber of He cryostat, by means of a planar spiral antenna and a Si immersion lens. A backward-wave oscillator, tunable throughout the spectral range, delivered an output power of few μW that was enough for optimum operation of the mixer. At 4.2 K ambient temperature and 1.025 THz radiation frequency, we obtained a receiver noise temperature of 1550 K despite of using a relatively noisy room-temperature amplifier at the intermediate frequency port. The noise temperature was fairly constant throughout the entire operation range and for intermediate frequencies from 1 GHz to 2 GHz.

INTRODUCTION

Astrophysical and stratospherical investigations in the terahertz (THz) frequency range, which are forthcoming events of the next few years, require heterodyne receivers with low-noise mixers. SIS mixers, having lowest noise temperatures up to ≈ 1 THz, have a drastic decrease in performance at higher frequencies. Sensitivity of Schottky diode mixers for THz range is limited by high intrinsic noise level in the diode. A superconductive hot-electron mixer (HEM), proposed in [1] and [2], is presently the only alternative to extend heterodyne spectroscopic measurements up to at least 10 THz, possibly over 30 THz. HEMs demonstrate a noise temperature, comparable to that of SIS receivers at 1 THz, and the lowest noise temperatures at higher frequencies [3]. They have also other advantages, like a small required local oscillator (LO) power, a nearly real impedance, and a relatively simple planar technology.

Two different ways to realize a HEM, with cooling of hot electrons via an out-diffusion of carriers from the sensitive element to contact pads [2], or by means of intensive electron-phonon interaction [1], result either in a smaller local oscillator power [3], or in a larger intermediate frequency (IF) bandwidth [4], respectively. Due to the lack of tunable LO sources in the far-infrared the large IF bandwidth is essentially important for spectroscopic measurements. Though future development of a tunable cw radiation source with a reasonable power at frequencies above 1.5 THz may weaken the latter requirement, IF bandwidth is currently an important issue for the THz mixer.

---

* E-mail: yuri@ele.kth.se

Large IF signal bandwidths, up to several GHz, of the phonon-cooled HEM have been realized with NbN due to a very short electron-phonon interaction time in this material, which is about 10 ps at 10 K [5]. Even a shorter time has been reported for Yba$_2$Cu$_3$O$_{7-\delta}$ [6], which could result in a high-temperature superconducting THz mixer with large IF bandwidth. Since the effective IF bandwidth of the hot-electron mixer is larger than the conversion gain bandwidth due to decrease of temperature fluctuation noise at high IF [7,4], NbN mixers are supposed to have effective IF bandwidths over 10 GHz.

In this paper we report on receiver measurements with an NbN phonon-cooled hot-electron mixer designed for operation in the THz range. Two devices have been investigated, with different sensitive element volumes and, correspondingly, different optimum LO power. We demonstrate that the receiver noise temperature is fairly constant between 0.9 THz and 1.2 THz throughout the IF measurements range.

EXPERIMENTAL SET-UP

35 Å thick NbN films were deposited on 350 μm thick Si substrates by magnetron spattering of Nb in the atmosphere of Ar and N; a 0.3 μm Ti-Au layer was deposited on top. By means of photolithography and ion milling a NbN microbridge and a gold planar logarithmic spiral antenna were formed (Fig. 1). Since NbN films have large sheet resistance, the microbridge was shaped in a horse shoe form in order to match the normal state resistance of the device to the radiation resistance of the planar antenna which is $377[2(\varepsilon+1)]^{-0.5} \approx 75\ \Omega$ ($\varepsilon = 11.4$ is the dielectric constant of Si). Arms of the planar antenna were connected to a co-planar transmission waveguide [8]. The superconducting transition temperature of NbN film for two devices used in the experiment was 7.5 K (device #1) and 7.9 K (device #2), with a transition width of 1.2 K and 1.1 K, respectively. The normal state resistance, taken at a temperature of 16 K, was 140 Ω for device #1 and 320 Ω for device #2.

A Si synthesized elliptical lens with no anti-reflection coating was used to couple radiation to the mixer. A hybrid antenna, consisting of the planar antenna and the immersion lens, had a nearly rotationally symmetrical radiation pattern (Fig. 2) with a main lobe width Θ_A of 1.7^0 at the −3 dB level. The radiation pattern was obtained by measuring a direct detection response of the NbN microbridge to a low power radiation at a frequency of 0.97 THz, produced by a backward-wave oscillator. The effective aperture of the hybrid antenna, ≈100 mm^2, was about 80 % of the cross-section of the immersion lens, thus approaching a maximum possible value.

Heterodyne measurements were performed with two black body radiation sources; a backward-wave oscillator (BWO), fabricated by ISTOK (Russia), served as a local oscillator at radiation frequencies between 0.9 and 1.2 THz. Maximum total output power, delivered by the BWO, was 10 μW at 0.97 THz. Two black body sources were placed in a vacuum chamber (Fig. 3), connected with a He cryostat, thus eliminating a problem of water vapor absorption in the signal path. One black body was attached to a metal can filled with liquid N$_2$ and had a temperature of about 90 K; the can was hanging in the vacuum chamber on a stainless steel tube serving also as a filling path for N$_2$. The

other black body was fixed to a wall of the vacuum chamber and had a temperature of 290 K.

A TPX lens, installed instead of one window of the vacuum chamber, was matching the diverging beam of the BWO to the hybrid antenna. A wire grid polarizer served as a beam splitter for device #1; a Mylar beam splitter was used when measuring with device #2. A Golay cell, calibrated with a black body radiation, was set in the LO path to control output power of the BWO. Black polyethylene film, cooled to 77 K, blocked the near-infrared background radiation from the vacuum chamber to eliminate parasitic heating of the mixer. A mechanical chopper with a gold-plated blade switched radiation from the two black bodies. IF signal from the mixer at frequencies between 1 GHz and 2 GHz was amplified by a room temperature amplifier (noise temperature 40 K), then integrated with a diode detector, and recorded by a lock-in amplifier. To measure the IF dependence of the noise temperature, we used an internal detector of HP8592L spectrum analyzer, thus having a possibility to measure the signal at different IF frequencies within the amplifier bandwidth; the resolution bandwidth was set to 3 MHz.

HETERODYNE MEASUREMENTS AND DISCUSSION

Current-voltage (IV) characteristics for both mixers with and without LO power applied are presented in Fig. 4. Dc resistance of both devices increased from a constant value of few Ω at bias voltage below 1 mV to about 30 Ω for device #1 and 60 Ω for device #2 at a bias of five millivolt. We apply the constant dc resistance at small bias voltage, R_s, to a dc series resistance of the bias tee (3.8 Ω) and the resistance of the spiral antenna arms. Device #2 demonstrated lower bias currents and higher differential resistance compared to those of device #1 within the bias voltage interval.

Optimum LO power, P_{LO}, absorbed by the mixer at a radiation frequency of 0.97 THz, was obtained as a difference between power, dissipated in the mixer at two operation points, 2 and 1, with and without LO applied, respectively. The dc resistance of the mixer at two points and, consequently, the electron temperature, was the same. We extracted the dc power dissipated in the series resistance R_s when calculating P_{LO}. Optimum LO power for device #2 (130 nW), was 6 times lower compared to that of device #1 (0.8 μW), corresponding to a smaller volume for the device #2. Since the available LO power was limited, we used the wire grid polarizer for heterodyne measurements with device #1, thus providing a larger LO power and having additional losses in the signal path. Besides 3 dB polarization loss in the signal path, the wire grid beam splitter added a resistive loss of 0.5 dB.

Double sideband (DSB) receiver noise temperature for different intermediate frequencies, measured with device #2 at 1.025 THz, is presented in Fig 5. Though the noise temperature varies within 10 % in the range of our IF amplifier, we could not observe any pronounced IF dependence. Deviations in the noise temperature should be rather explained by the influence of our IF chain.

Noise temperature versus radiation frequency for device #2 is presented in Fig. 6. The noise temperature is fairly constant throughout the operation range. The largest Y-

factor, 1.122, and a corresponding noise temperature of 1550 K were obtained at 1.025 THz for an IF of 1.1 GHz. We should point out that all measurements were performed with a room temperature IF amplifier, which contributes about 30 % to the total noise temperature of the receiver. Using a cooled amplifier should result a decrease in noise temperature down to $\approx$ 1000 K.

Device #1 demonstrated a higher noise temperature (Fig. 6). However, unlike device #2, it was used with the wire grid beam splitter, which had much higher losses compared to that of the Mylar beam splitter. Extracting 3.5 dB loss in the grid beam splitter, we obtain a lowest noise temperature of 1170 K at 0.97 THz, which is less than that of device #2 with extracted losses in Mylar. The lower noise temperature of device #1 may be explained by a smaller normal state resistance, resulting in a smaller rf mismatch.

Other rf losses, which contribute to the receiver noise temperature, are listed in Table 1. Extracting reflection loss at the surface of the immersion lens, reflection and transmission loss in the polyethylene filter, and contribution from the IF amplifier, we obtain a 300 K intrinsic noise temperature of the mixer. Better matching a rf and IF impedance would result in even lower noise temperatures.

Table 1. Rf losses

Element	Loss (dB)	
	Device #1	Device #2
Beam Splitter (wire grid)	3.5	-
Beam Splitter (Mylar)	-	1
Black Polyethylene filter	0.5	0.5
Reflection at Si surface	1.5	1.5
Absorption in Si	0.4	0.4
Rf mismatch	0.4	2.1

The measured low value of the system noise temperature of the NbN phonon-cooled hot-electron mixer and obvious possibilities for further improvement demonstrate the advantages of the mixer at THz frequencies. Comparing our present results with those obtained in the first experiments with phonon-cooled HEM at 2.5 THz [9], where the noise temperature was many times higher, one should find a reasonable explanation for a drastic decrease in sensitivity at the higher frequency. We should mention numerous changes in our present experimental setup, such as better quasi-optical alignment of the system, eliminating the problem of water vapor absorption, and much higher power stability of the BWO compared to that of the FIR gas laser used in [9]. As a one more important factor, we should point out a greatly improved quality of NbN films. We believe there is no physical reason for any deterioration in performance at radiation frequencies up to at least 10 THz.

CONCLUSION

We have shown operation of NbN hot-electron mixer in a frequency range between 0.9 and 1.2 THz without any deterioration in performance. The measured DSB receiver noise temperature, about 1550 K, only slightly changes at intermediate frequencies from 1 GHz to 2 GHz, thus proving a suitability of phonon-cooled hot-electron mixers for spectroscopic measurements.

ACKNOWLEDGMENTS

REFERENCES

1. E. M. Gershenzon, G. N. Gol'tsman, I. G. Goghidze, Yu. P. Gousev, A. I. Elant'ev, B. S. Karasik, and A. D. Semenov, The mixer for millimeter and submillimeter wavelengths based on electron heating in the resistive state of superconductive films, *Sov. Phys. Superconductivity* **3**(10), pp. 1582-1597 (1990).
2. D.E. Prober, Superconducting terahertz mixer using a transition-edge microbolometer, *Appl. Phys. Lett.* **62**(17), pp. 2119-2121 (1993)
3. B.S. Karasik, M.C. Gaidis, W.R. McGrath, B. Bumble, and H.G. LeDuc, Low noise in a diffusion-cooled hot-electron mixer at 2.5 THz, *Appl. Phys. Lett.* **71**(11), pp. 1567-1569 (1997).
4. H. Ekström, E. Kollberg, P. Yagoubov, G. Goltsman, E. Gershenzon, and S. Yngvesson, Gain and noise bandwidth of NbN hot-electron bolometric mixers, *Appl. Phys. Lett.* **70**(24), pp. 3296-3298 (1997).
5. Yu.P. Gousev, G.N. Gol'tsman, A.D. Semenov, E.M. Gershenzon, R.S. Nebosis, M.A. Heusinger, and K.F. Renk, Broadband ultrafast superconducting NbN detector for electromagnetic radiation, *J. Appl. Phys.* **75**(7), pp. 3695-3697 (1994).
6. A.D. Semenov, R.S. Nebosis, Yu.P. Gousev, M.A. Heusinger, and K.F. Renk, Analysis of the nonequilibrium photoresponse of superconducting films to pulsed radiation by use of a two-temperature model, *Phys. Rew. B* **52**(1), pp. 581-590 (1995).
7. B.S. Karasik and A.I. Elantiev, Noise temperature limit of a superconducting hot-electron bolometer mixer, *Appl. Phys. Lett.* **68**(6), pp. 853-855 (1996).
8. Yu.P. Gousev, A.D. Semenov, E.V. Pechen, A.V. Varlashkin, R.S. Nebosis, and K.F. Renk, Coupling of THz radiation to a high-T_c superconducting hot electron bolometer mixer, *Appl. Phys. Lett.* **69**(5), pp. 691-693 (1996).
9. A. D. Semenov, Yu. P. Gousev, R. S. Nebosis, K. F. Renk, P. Yagoubov, B. M. Voronov, G. N. Gol'tsman, and E. M. Gershenzon. Heterodyne detection of THz radiation with a superconducting hot-electron bolometer mixer. *Appl. Phys. Lett.* **69**(2), pp. 260-262 (1996).
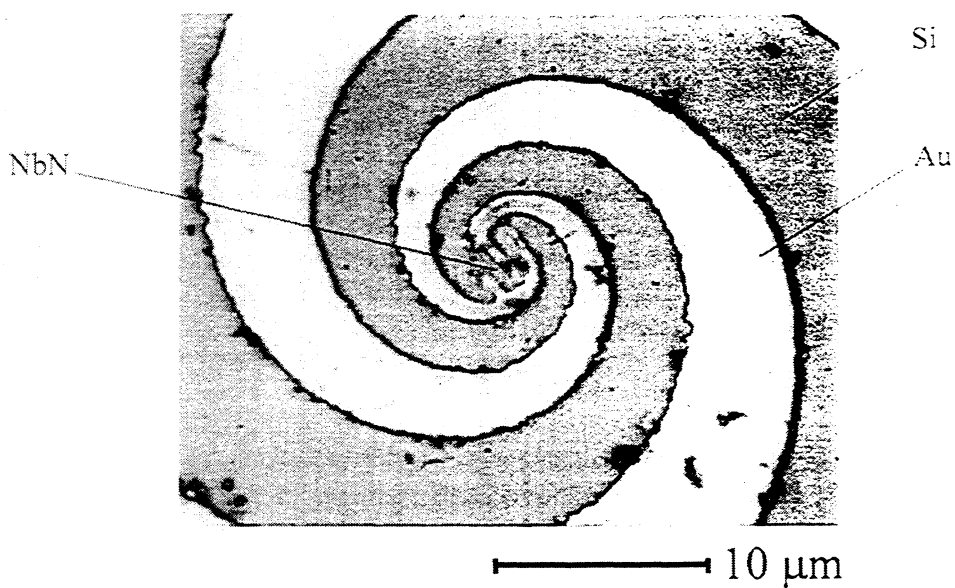
Fig. 1. Inner part of the planar spiral antenna. The NbN film between the
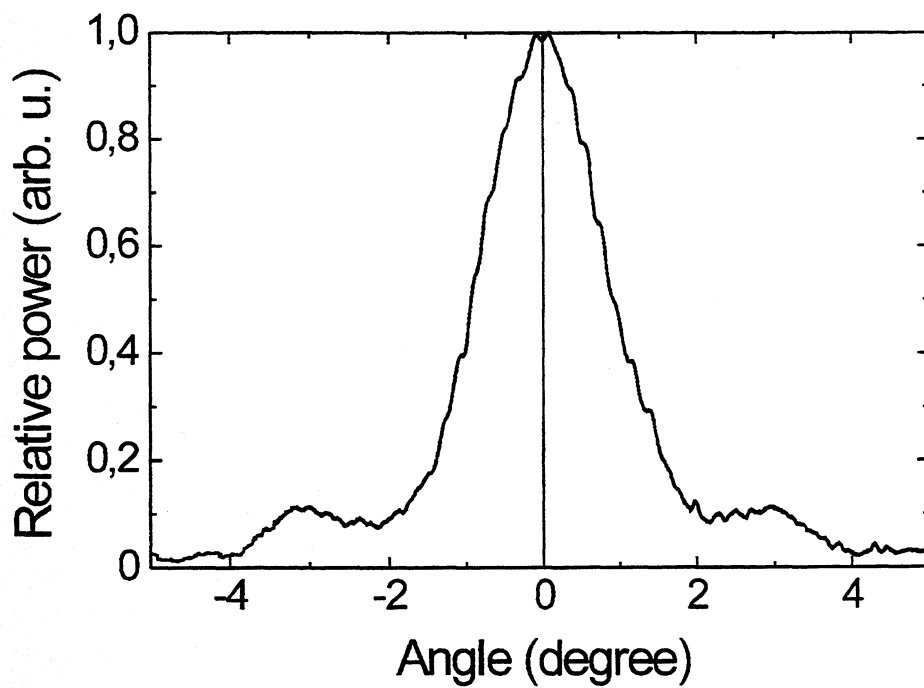antenna arms is transparent and therefore not visible on the picture.

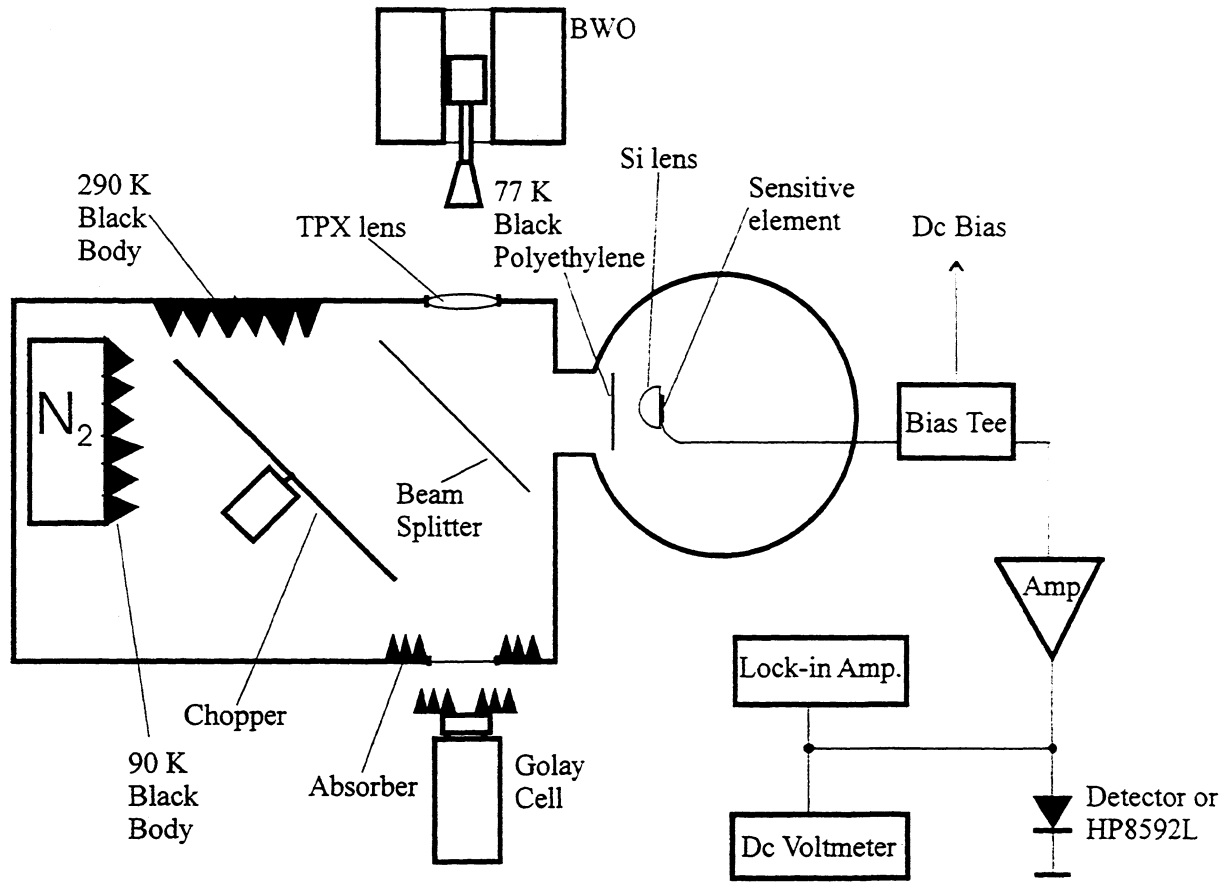Fig. 2. Radiation pattern of the hybrid antenna at 0.97 THz.

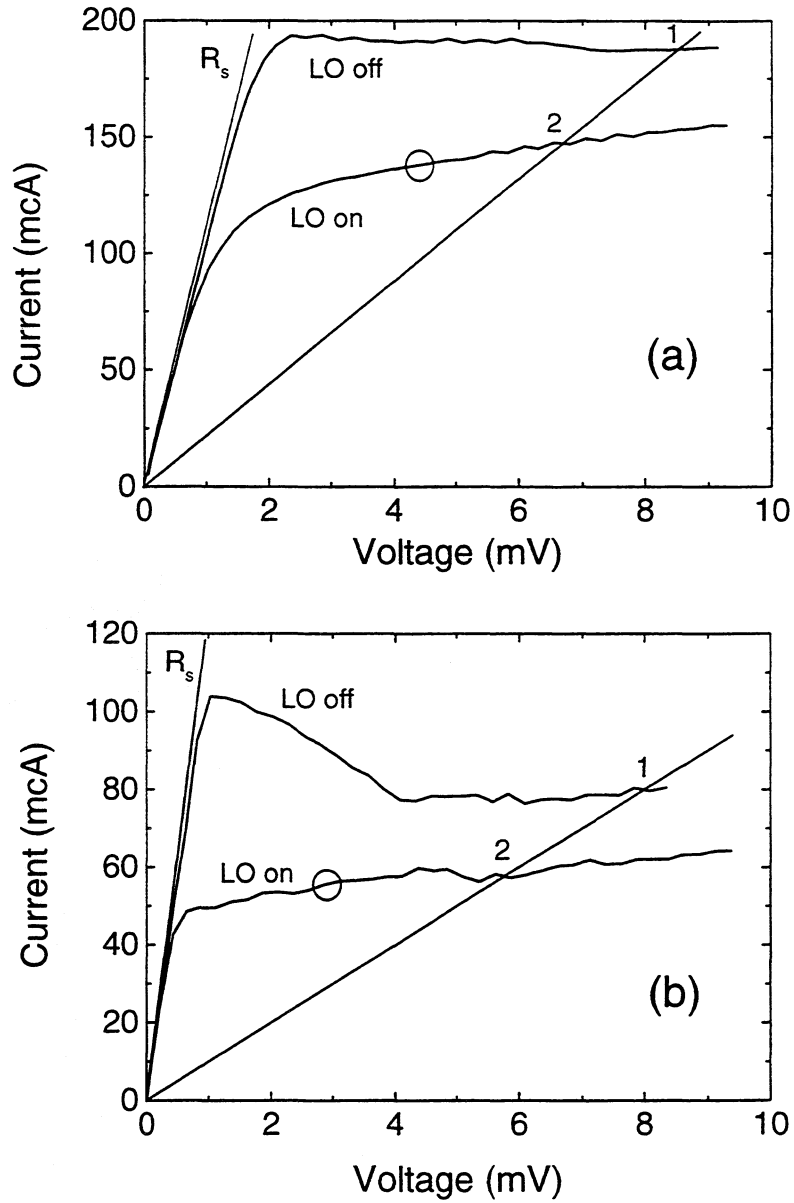Fig. 3. Block diagram of the experimental set-up.

Fig. 4. Voltage-current characteristics for device #1 at an ambient temperature of 3.9 K (a) and device #2 at a temperature of 4.2 K (b). Operation point is marked by a circle.
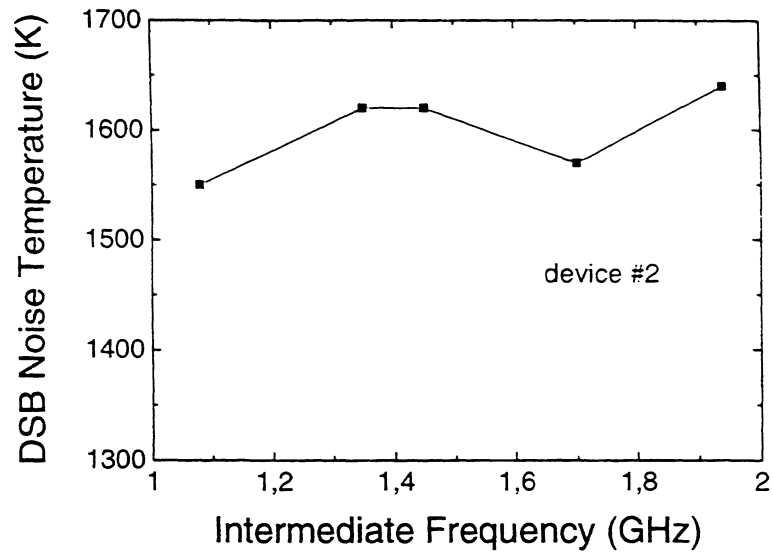
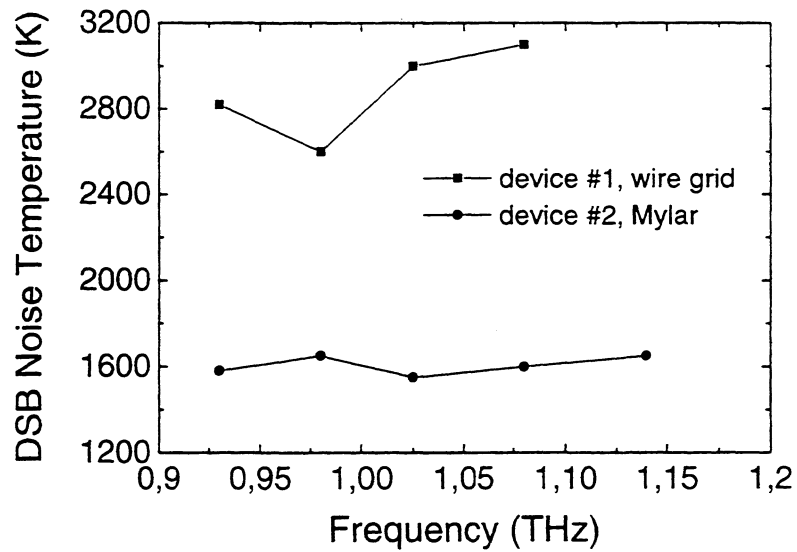Fig. 5. System noise temperature versus intermediate frequency
for device #2.

Fig. 6. System noise temperature for different radiation frequencies.

129